Journal of Thermal Analysis and Calorimetry, Vol. 59 (2000) 337–350

Dedicated to Prof. Edith A. Turi in recognition of her leadership in education

EXPANSION AND SHRINKAGE OF FIBERS
Load- and temperature modulated TMA measurements temperature calibration of fiber attachments

R. Riesen and J. E. K. Schawe*

Mettler-Toledo GmbH, Sonnenbergstrasse 74, CH-8603 Schwerzenbach, Switzerland

Abstract

The thermal behavior of a drawn PET fiber has been investigated by thermomechanical analysis, TMA, and by differential scanning calorimetry, DSC. Above the glass transition temperature of 79°C, the fiber shrinks to a maximum of 8% of the initial length. Temperature modulated TMA enabled the separation of the thermal expansion from the overlapping shrinkage during the first heating and to calculate the expansivity, α_e and the shrinkage coefficient, α_s, independent of each other. Young's modulus, *E*, was measured by TMA with modulation of the tensile stress. Hence, it was possible to record the behavior of α_e, α_s and *E* during the structural changes by combining both modulations in a single measurement.

A new technique was developed to calibrate the sample temperature. With this, accurate control of the modulated temperature of the specimen was achieved, independent of the changing heating rate.

Keywords: expansivity, fibers, modulus, shrinkage, temperature calibration, temperature modulation, thermomechanical analysis, TMA

Introduction

The uniqueness of fibers lies in their anisotropy mainly due to the spinning and drawing process during production [1, 2]. As a result, many of the physical properties depend on the mechanical and thermal treatment and hence, are subject of thermoanalytical characterization, e.g. by thermomechanical analysis (TMA). This is even more demanding due to the fact, that such polymer systems may be far above equilibrium [3] with metastable phases and time dependent transitions. Thermal shrinkage is an important characteristic property which reflects the process history of fibers [2]. It is measured by classical TMA using constant heating rate and constant tensile load. In the same way the coefficient of thermal expansion, α_e, of a non-shrinking sample is recorded. Young's modulus (*E*) also can be measured by TMA applying alternating load changes during heating [4].

* Author for correspondence: e-mail: rudolf.riesen@mt.com

1418–2874/2000/ $ 5.00

Akadémiai Kiadó, Budapest
Kluwer Academic Publishers, Dordrecht

But, with drawn fibers, the expansion is superimposed by the shrinkage and is therefore not accessible by conventional TMA. Expansivity and shrinkage are physically coupled by the structure and hence, both change during structural relaxation. However, each property is controlled by different effects (e.g. free volume, crystal perfection) and show different time behavior. Additionally, the shrinkage is influenced by non-reversible changes of the internal stress. The expansivity is not the same before and after shrinkage. Therefore, α_e of a drawn fiber can not be determined by a second heating.

A new technique to separate the thermal expansion and the shrinkage behavior is the temperature modulated TMA [5, 6]. In this technique, the mean heating rate is superimposed by a modulated heating rate to give rather short and small temperature changes if compared to the total temperature rise. For example, the sample temperature oscillates in a sine form at a maximum rate of 5 K min^{-1} and a minimum rate –4 K min^{-1} within period of 3 min and gives a mean heating rate of 1 K min^{-1}. A shrinkage process due to the mean temperature increase is slow and not reversible. But, the normal thermal expansion is reversible and follows the short temperature changes. Therefore, α_e can be measured by the short term length changes unaffected by the simultaneous slow length changes of the shrinking process with its coefficient, α_s.

Young's modulus, *E*, can be measured using a modulation of the tensile stress. If this frequency is enough different from the temperature modulation, both modulations can be applied simultaneously. Fourier-analysis of the resulting TMA curve allows to calculate the *E*, α_e and α_s from one measurement of the same specimen.

Temperature modulated TMA requires the sample temperature to follow the applied heating rates. Due to the necessary temperature gradients in the furnace a thermocouple close-by the fiber may not be equal to the sample temperature. Therefore, a new technique to record and calibrate the sample temperature has to be developed.

Theory

Expansivity

Structural changes take place during temperature increase and may give dramatic changes to the apparent expansivity, α^*_e. Especially, drawn fibers exhibit a large shrinkage during the first heating. The relation between the length change, heating rate and α^*_e is given in Eq. (1).

$$\alpha^*_e = (\mathrm{d}l/\mathrm{d}T)/l_0 = \nu/(\beta l_0) \tag{1}$$

l – length, T – temperature, l_0 – initial sample length, t – time, $\nu = \mathrm{d}l/\mathrm{d}t$ rate of length change, $\beta = \mathrm{d}T/\mathrm{d}t$ heating rate.

The apparent expansion of fibers measured by TMA can be split up in a reversible part controlled by the coefficient of expansion, α_e and an irreversible part given by a coefficient of shrinkage, α_s.

$$\alpha^*_e = \alpha_e + \alpha_s \tag{2}$$

Exactly in analogy to the techniques used in temperature-modulated DSC [7–9] temperature-modulated TMA can be applied to separate these two coefficients from each other. Instead of constant heating rate, a sine wave is modulated on a low mean heating rate, β_{mean}:

$$T(t)=T_0+\beta_{mean}t+T_A\sin(\omega t) \quad (3)$$

T_0 – start temperature, T_A – amplitude of the temperature modulation, $\omega=2\pi/p$ – angular frequency, p – the period of the modulation.

By differentiation of Eq. (3) the instantaneous heating rate, $\beta(t)$, is given by the following equation:

$$\beta(t)=\beta_{mean}+\beta_A\cos(\omega t) \quad (4)$$

β_A – amplitude of the heating rate.

Measuring the TMA signal a modulated rate of length change, ν, is recorded with the mean value ν_{mean} and the amplitude ν_A:

$$\nu=dl/dt=\nu_{mean}+\nu_A\cos(\omega t-\varphi) \quad (5)$$

φ – phase shift.

The relaxation process is usually slow and mainly time controlled compared to the temperature modulation periods. But, the normal linear expansion is able to follow the modulation program. Therefore, ν can be split into two parts (see also Eq. 2).

$$\nu=\alpha^*_e\beta_{mean}+\alpha_e\beta(t) \quad (6)$$

Similar to Eq. (1), α_e can be calculated from the amplitude of the rate of length change, ν_A, and the amplitude of the instantaneous heating rate, β_A:

$$\alpha_e=\nu_A/(\beta_A l_0) \quad (7)$$

The amplitude ν_A can be calculated from the measured curve ν using Fourier analysis. If the sample temperature follows the superimposed modulation, the amplitude of the heating rate equals the programmed amplitude. At low temperatures, or if the sample doesn't follow the modulation due to lack of temperature lag compensation, the amplitude can be calculated from the sample temperature measured very close to the fiber. Again, Fourier analysis is used to calculate the mean and amplitude.

In general, frequency dependent material parameters (i.e. α_e) can be treated as complex values. However, it can also be assumed that the real part of the complex expansivity is much larger than the imaginary part. Therefore, the imaginary part has not been considered in this investigation. In addition to that, a phase shift between the modulated heating rate and the resulting TMA signal is namely due to heat transport phenomena so that the actual imaginary part of α_e is not measurable.

The apparent expansivity α^*_e is calculated from the corresponding mean of the ν signal, ν_{mean}. Again, β_{mean} can be taken from the mean heating rate or in case of control problems from the Fourier analysis of the measured heating rate:

$$\alpha^*_e = \nu_{mean}/(\beta_{mean} l_0) \quad (8)$$

The coefficient of shrinkage, α_s is the difference between apparent expansivity and α_e (Eq. (2)).

Young's modulus

Young's modulus, E, is determined from the relation of the applied tensile stress to the corresponding strain. The temperature dependence of E during and after the shrinkage of fibers will be calculated according to Eq. (9) using Fourier analysis of the TMA curve. In the following, E refers to storage modulus.

$$E = (\Delta F/\Phi)/(\Delta l/l_0) \quad (9)$$

ΔF – change of the tensile force (load change in the TMA experiment), Φ – cross section area of the fiber, Δl – corresponding length change, l_0 – actual length of the fiber. It is assumed, that Δl is very small compared to l_0.

Temperature calibration

The correct calibration of the actual temperature of the fiber is a crucial condition to get accurate values. This can be difficult due to the distance between sample and temperature sensor. Additionally, the samples can be used only once and reference substances are unavailable. And, if the dependence on temperature, heating rate and purge gas type has to be considered it is getting even more complex. All this is of special importance in connection with temperature-modulation techniques.

To be able to control the sample temperature accurately, the thermal lag between the furnace (with embedded thermocouple, T_c) and the sample itself, T_s, has to be known, i.e. has to be calibrated. There is also a temperature difference between the thermocouple close to the sample and the sample itself. The related temperature gradients are depending namely on the heating rate, the purge gas type and the heat capacities e.g. of the sample support. The temperature difference between furnace and sample is called temperature lag and is described as follows:

$$T_c - T_s = \Delta T_{lag} = \beta\tau_{lag} \quad (10)$$

τ_{lag} is a time constant describing the rate of temperature equilibration and is depending on experimental parameters such as the nature of the purge gas, the furnace or the heat capacity of the sample.

Hence, a new technique with standard reference materials (e.g. indium) linked to the fiber uses the conventional onset of melting measured by SDTA. The SDTA signal is the temperature difference between the sample temperature and the program temperature if temperature control includes the calibrated lag. Reusable samples enable for easy repetition of measurements and automated procedures. The FlexCal™ concept allows to determine and store all necessary calibration parameters [10].

In certain cases the TMA curve is also affected by the melting and hence, can be used for temperature calibration too.

Experimental

Measurements were carried out on a METTLER TOLEDO STAR[e] System with TMA/SDTA 840, DSC821[e] and the respective software packages. The fibers of poly(ethylene terephthalate), PET, (Viscosuisse Typ 260, 108 dtex, 0.10 mm diameter) were mounted by copper clamps at the fiber attachment giving a standard length of 13 mm. The expansion of the copper clamps (equivalent to 1 mm) and the fused silica hooks is compensated by the software.

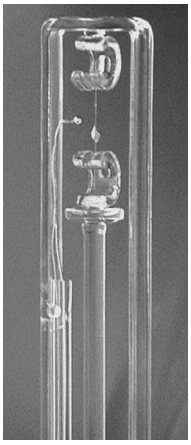

Fig. 1 Sample arrangement in the fiber attachment kit with an indium pellet mounted a little below the center

To check the sample temperature, an indium pellet (99.999% purity, approx. 6 mg) was cut into two pieces, flattened and pressed onto the center of the PET fiber from both sides with the fiber in-between (Fig. 1). All these measurements with indium were performed with preheated fibers. The thermocouple to measure the temperature close to the fiber was placed towards the center of the fiber, 3 mm in distance.

The measuring programs were as follows:

a) Measurement of the melting of indium attached to the fiber: 100 to 200°C at a rate of 10 K min^{-1}; atmosphere: static air.

b) Modulation measurements: 30 to 230°C at a mean rate of 1 K min^{-1} with 2°C amplitude at periods of 3 min; load to the fiber: alternating between 0.05 and 0.07 N at a period of 10 s. Rather large amplitudes were needed for accurate determination of small expansivities.

The use of other conditions or deviations from the above parameters are given with the respective results, if necessary.

Temperature calibration

Prior to the measurements, the TMA module was calibrated with respect to temperature and τ_{lag} according to the standard procedure given by the system. An arrangement as shown in Fig. 1 was used, which allowed repetitive measurements at different heating rates using the same specimen (refer to Eq. (10)). The measuring signals (length change by TMA, temperature change by SDTA) for a heating and cooling run are shown in Fig. 2. The SDTA records the melting and the crystallization peak of the indium and the onset is taken as the melting point. The TMA curve shows similar, but very small peaks, due to the fact that the rate of expansion or contraction of the fiber is reduced: the part of the fiber covered by the indium stays at 156.6°C during the process of melting and does not add to the expansion. Due to the slow heat transfer through the purge gas, the melting peak is rather broad. Nevertheless, the onset in the SDTA peak is clearly defined, whereas the corresponding onset on the TMA curve is detected often not clearly enough.

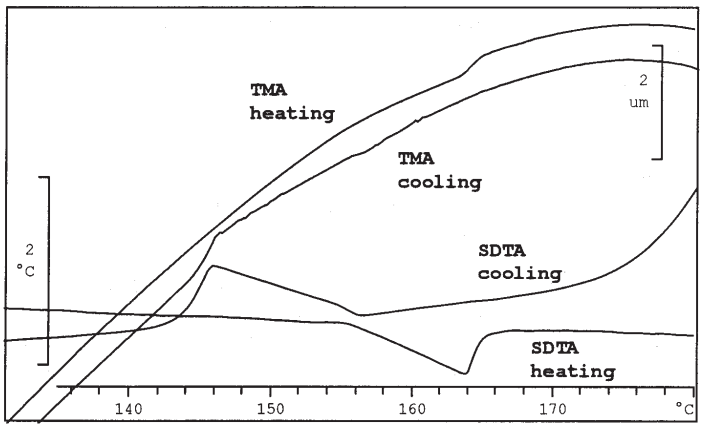

Fig. 2 TMA and SDTA curves of the PET fiber with pellet of indium similar to Fig. 1. Cooling rate: 5 K min^{-1}. Exothermic direction upwards

The reproducibility of five measurements using the same specimen is characterized by the following standard deviation: onset TMA=0.27 K, onset SDTA=0.15 K, peak SDTA=0.05 K and integral SDTA=0.72 Ks. The best reproducibility is achieved at the endpoint of melting (SDTA Peak). The onset of the SDTA peak is the intersection point of the tangents and hence, is slightly at higher temperatures than the onsets on the TMA curves. But, the onsets of the SDTA peaks are better reproducible. The use of helium instead of air lowers the measured onset temperatures due to the better heat transfer. For both gases, a slight increase of the onset is observed between the first heating of the freshly prepared sample and the subsequent measurement. This is mainly due to the shape of the SDTA peak giving different extrapolated onset values.

A mass dependence of the melting onset could not be measured, but the peak size is reduced with decreasing mass, as it is also observed also with DSC measurements. Hence, it can be assumed that temperature calibration by the onset value is independent of the In-sample mass used (typically 5 to 10 mg In).

The temperature depends on the nature of the furnace atmosphere due to the rate of heat transfer. But, the gas flow rate has practically no influence as it is shown in Table 1. That means, there is no additional cooling by the purge gas flow during the temperature scans.

Table 1 Influence of the gas flow rate: measurements of the characteristic values of the SDTA peak of melting of 6.18 mg of indium

Flow rate of air/ ml min^{-1}	Onset SDTA/°C	Peak SDTA/°C	Integral SDTA/Ks
50	155.7	167.5	19.4
50	156.1	167.5	17.8
100	156.4	167.7	19.6
100	156.4	167.5	18.8
150	156.4	167.7	18.2
200	157.0	167.8	18.0
200	156.7	167.8	18.2
250	156.9	168.0	18.7
Mean	156.44	167.69	18.58
Standard deviation	0.42/K	0.19/K	0.66/Ks

Table 2 Measurements of the characteristic values of the SDTA peak of melting of 6.21 mg of indium attached to the center of a fiber loop with the indicated horizontal distances to the thermocouple. The fiber loop was hooked-in in different places to give the various distances of the indium pellet to the thermocouple

Distance/mm	Onset SDTA/°C	Peak SDTA/°C	Integral SDTA/Ks
0.5	157.1	167.7	70.6
2.0	154.9	166.0	29.6
3.5	154.2	165.7	15.2
5.0	154.2	163.5	7.1

The distance between the indium pellet and the thermocouple, measuring the SDTA signal, has a big influence on the peak size but much less on the temperatures measured. An increasing distance leads to reduced SDTA sensitivity of thermal effects on the fiber (Table 2).

With correct calibration of τ_{lag} the onset of the SDTA peak is independent on the heating rate, as it is shown in Fig. 3 and listed in Table 3. A value of 91 s has been determined for τ_{lag} . The melting can be detected even at the low heating rate of

0.2 K min^{-1}. Extrapolated onset values are given in Table 3, also for heating rates not shown in Fig. 3.

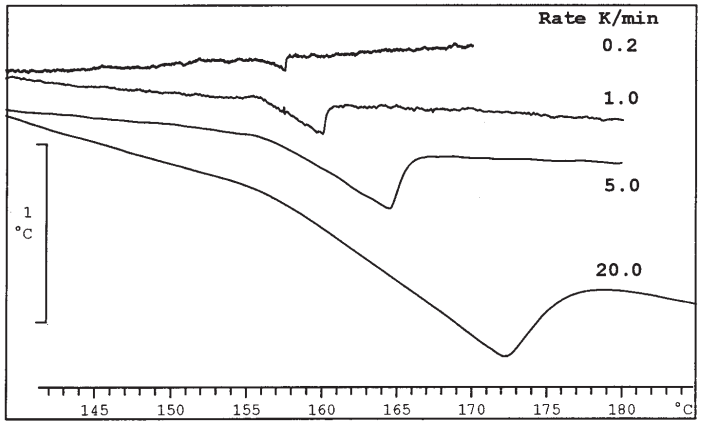

Fig. 3 SDTA curves of the PET fiber with mounted In-pellet at heating rates from 0.2 to 20 K min^{-1}. Exothermic direction upwards

Table 3 Onset temperatures of the SDTA peaks of the indium melt for different heating rates

Heating rate/K min^{-1}	Onset SDTA/°C
0.2	156.1
0.5	156.3
1.0	156.1
2.5	156.2
5.0	155.9
10.0	156.6
20.0	156.4
Mean	156.22
Standard deviation	0.20/K

Results of simultaneous measurements of modulus and expansivity

The thermal behavior of the PET fiber under investigation during the first and second linear heating is shown in Fig. 4. The shrinkage recorded by TMA starts right after the glass transition temperature of 79°C and amounts to 8.1%. The cold crystallization starts also after glass transition with a heat of crystallization of 13.8 J g^{-1} measured by DSC. The heat of melting is 52.4 J g^{-1}. During the second heating the expansion starts at 106°C followed by a small shrinking just before the sample softens due to melting. No significant further cold crystallization could be measured.

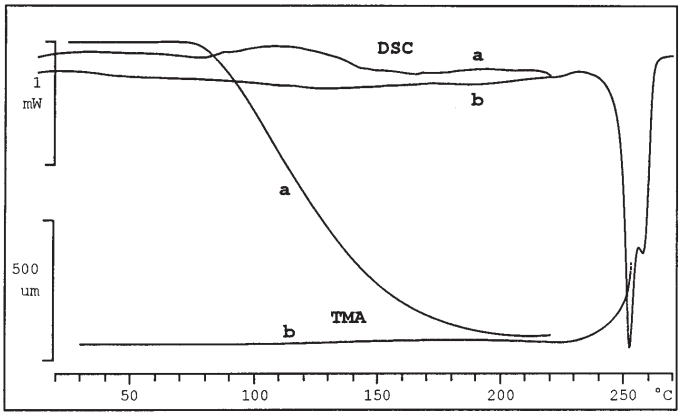

Fig. 4 Conventional TMA and DSC curves of the PET fiber recorded in a first heating (a) up to 220°C and in a second heating (b) to 270°C with normal cooling in-between. DSC: 2.51 mg in 20 µl aluminum pan; TMA: 13 mm fiber with a tensile load of 0.1 N. 50 ml min^{-1} nitrogen purge. Heating rate: 10 K min^{-1}. Exothermic direction upwards

To separate the expansion from the shrinkage, the PET fiber was measured in the TMA with the temperature-modulation as shown in Fig. 5. In addition to this a load modulation is superimposed at the same time, with the tensile force alternating between 0.05 and 0.07 N every 5 s (Fig. 5). The two modulations are well visible on both TMA curves, especially during the shrinkage. The shrinkage does not stop during the short cooling periods and would come to an equilibrium only after a long isothermal period.

The length changes due to the sudden load changes (Fig. 5) are evaluated according to Eq. (9) to determine the behavior of the storage modulus, *E*. Figure 6 shows the complete TMA curves (upper coordinates) and the respective curves of *E*

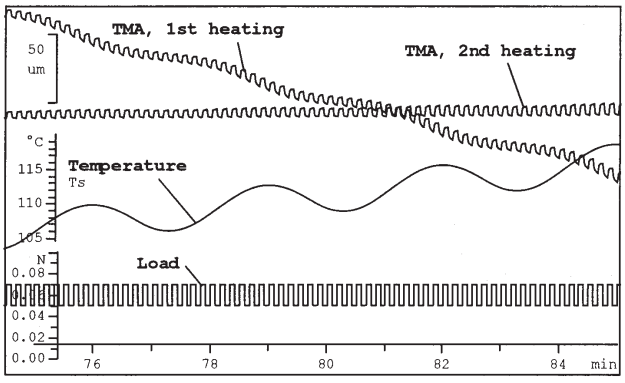

Fig. 5 TMA curves of the PET fiber measured by load and temperature modulation in a first and second heating up to 220°C with normal cooling in-between. For better view of the modulation, the curves are shown only in the temperature range of 105 to 115°C

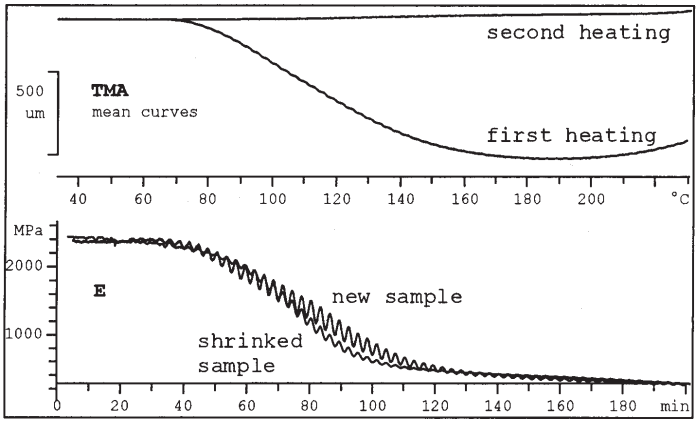

Fig. 6 TMA curves of the PET fiber (mean of the load-modulated curves shown in Fig. 5). *E* is calculated by Fourier analysis from the load-modulated TMA curves and is plotted in function of time for the same temperature range. Mean heating rate: 1 K min^{-1}

(lower coordinates) for the first heating (new sample) and the second heating (shrinked sample). *E* has approximately the same values for the original and the shrinked sample, but the temperature dependence during shrinkage process is much more pronounced if compared to the second heating, i.e. after further crystal perfection. The value of *E* follows the temperature modulation, especially in the range above the glass transition temperature up to the end of shrinkage. *E* decreases dramatically above the glass transition of the residual amorphous parts.

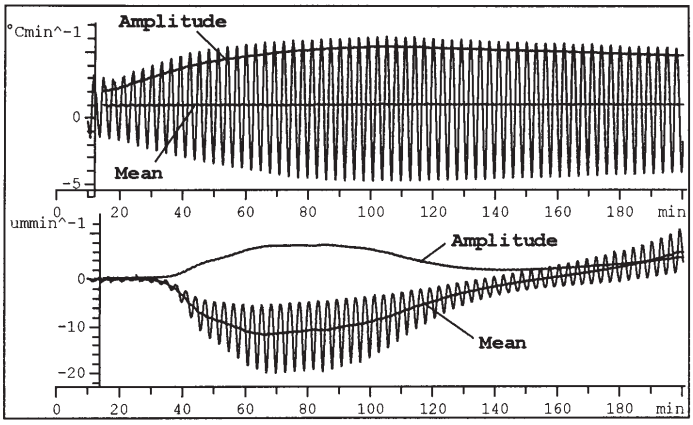

Fig. 7 Upper coordinates: derivative of the sample temperature (β) of the PET fiber during the first heating. Lower coordinates: derivative of temperature modulated TMA curve (ν) with load modulation filtered out. Using Fourier analysis, the mean of the modulated curves (β_{mean}, ν_{mean}) and the amplitudes (β_A, ν_A) are calculated in each coordinate. The initial TMA curve is shown in Fig. 6

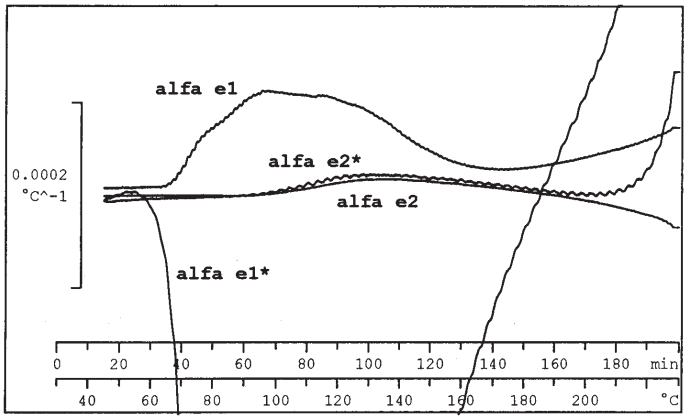

Fig. 8 PET expansivity curves derived from the curves shown in Fig. 7. The ordinate is scaled to $°C^{-1}$, equivalent to μm/(m °C), for the values of α_e and α_e^*) each for a 1st and a 2nd heating

The derivatives of the sample temperature (β, β_{mean} and β_A) and the derivatives of the respective TMA curves (ν, ν_{mean} and ν_A) are shown in Fig. 7 and are being used to calculate the coefficients of expansion and shrinkage according to the equations given in the theory.

The coefficient of expansion, α_e, is calculated using the curves of the amplitudes (Eq. (7)) and the apparent expansivity α_e^* is calculated dividing the mean curves (Eq. (8)). The calculated curves are shown in Fig. 8. The coefficients of expansion are calculated for the first (index 1) and second heating (index 2) of the same specimen.

Figure 9 shows the coefficient of shrinkage, $\alpha_s = \alpha_e^* - \alpha_e$, for the first and second heating, calculated from the curves in Fig. 8. During the first heating the coefficient of shrinkage, α_{s1}, dominates the expansivity, α_{e1}. Nevertheless, α_{e1} is increasing during the shrinkage process due to the increase of the free volume [11, 12] of the amorphous phase. Two processes contribute to the increase of the free volume: first the glass transition and second the additional structural relaxation. Above 100°C cold crystallization takes place (see also Fig. 4) reducing the amorphous amount and with this also α_{e1}. At higher temperatures the material re-crystallizes leading to a further change of α_{e1}. The maximum temperature reached was 230°C, well below the melting (Fig. 4).

At the beginning of the second heating, α_{e2} is small. Passing the glass transition α_{e2} increases. Rising the temperature above 180°C α_{e2} is reduced and turns even into negative. It has to be noted that α_e always is referring only to the fiber direction and does not consider total volume changes.

Comparison of α_{e2}, measured by temperature-modulated TMA, with the apparent expansivity calculated from the non-modulated curve (TMA curve b, Fig. 4) shows exactly the same behavior, i.e. the values at 50°C are approximately zero but increase to $20 \cdot 10^{-6}$ $°C^{-1}$ at 130°C.

No shrinkage occurs during second heating. Hence, α^*_{e2} is expected to be equal to α_{e2} within the measuring tolerance, as it is shown in Fig. 8 up to 170°C. Above this temperature, the sample starts to flow giving an increase of α^*_{e2}.

The coefficient of shrinkage, α_s (Fig. 9), shows the rate of irreversible contraction of the fiber above glass transition. Close to the melting region the irreversible length change turns into an elongation due to loss of tie molecules [13]. There is a small creeping revealed by the positive values of α_s during the second heating.

The rates of the respective changes of expansivity and shrinkage are different despite of the fact, that both properties are physically coupled by the structure. This is shown in a quasi-isothermal experiment at 110°C after reaching this temperature at a rate of 1 K min^{-1} (temperature modulation in the isothermal phase as in the previous cases). Figure 10 shows the time dependence of the total sample length, l_{mean}, and the length amplitude, l_A. The time evaluation of both values can be described by a stretched exponential function [14]:

$$l=l_\infty+l_i\exp\{-(t/\tau)^\gamma\} \quad (11)$$

The characteristic time, τ, of the overall shrinkage is about 3 times larger than that of the α_e-relaxation. The width of a relaxation process is characterized by the stretching parameter γ. For the overall shrinkage γ is much smaller than for the α_e-relaxation (Table 4). As a result, the dynamic behavior of both relaxation processes is different: the stretching parameter γ is for the shrinkage (l_{mean}) much smaller than for l_A describing a very long tailing, as the fitting parameters in Table 4 show.

Table 4 Behavior of expansivity and shrinkage as measured by a temperature modulated TMA experiment under quasi isothermal conditions at 110°C. Fitting parameters of the curves in Fig. 9, as discussed in the text

	l_∞/μm	l_i/μm	τ/s	γ
l_{mean}	12464	242	960	0.23
l_A	0.228	1.827	319	0.8

Conclusions

With temperature modulated TMA it is possible to separate thermal expansion and shrinkage during a relaxation process of drawn fibers. Since the modulation frequencies for the measurement of the tensile modulus and the expansivity can be different by a factor of 10, it is now easily possible to apply force and temperature modulation simultaneously during a slow underlying temperature increase. Therefore, a single TMA measurement provides all these temperature dependent properties of a fiber to study influences of draw ratio or other influences of thermal or mechanical treatment.

Accurate control of the sample temperature modulation made it necessary to develop a new technique to check the temperature. Standard reference materials (e.g. indium) are attached to the fiber to measure in a conventional way the onset of melting recorded by the SDTA. The SDTA signal is the temperature difference between

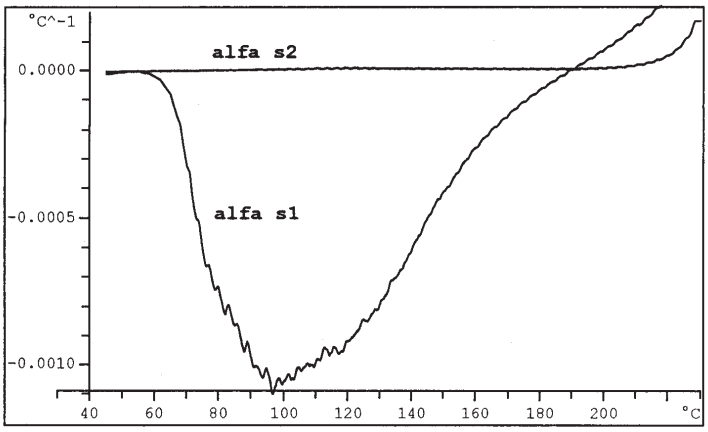

Fig. 9 Shrinkage coefficients of the first (alfa s1=α_{s1}) and the second (alfa s2=α_{s2}) heating calculated from the curves shown in Fig. 8

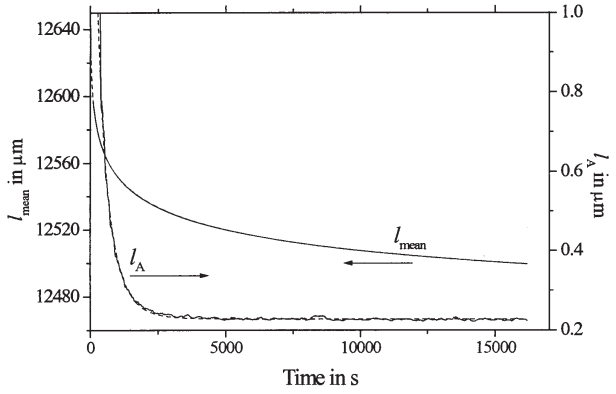

Fig. 10 Shrinkage of a PET fiber after heating to 110°C, measured quasi isothermally by temperature-modulation TMA (start temperature: 50°C, heating rate: 1 K min^{-1}, amplitude: 2 K, period: 3 min, initial length of PET fiber: 13 mm, constant load of 0.06 N). l_{mean} represents the mean of the resulting modulated TMA curve, l_A is the amplitude of it, both in function of the isothermal holding time (time scale is corrected for the heating period)

the temperature measured closely to the sample and the program temperature under calibrated conditions. Reusable samples allow for repeated measurements and automated procedures. The recorded melting points are highly reproducible and are well suited for calibration purposes.

The SDTA measures larger endothermic or exothermic effects even of samples small as single fibers.

The described techniques can also be applied to samples other than fibers, e.g. solids in the penetration or expansion mode, in the bending arrangement or in cases of swelling measurements.

References

1 L. H. Sperling, Introduction to physical polymer science, 2nd ed., Wiley-Interscience, New York 1992, p. 263.
2 M. Jaffe, Thermal Characterization of Polymeric Materials, 2nd Ed., E. A. Turi, ed., Academic Press, New York 1997, p. 1767.
3 B. Wunderlich, J. Thermal Anal., 46 (1996) 667.
4 H. G. Wiedemann, R. Riesen and A. Boller, ASTM STP 1136, American Society for Testing and Materials, Philadelphia 1991, p. 84.
5 D. M. Price, J. Therm. Anal. Cal., 51 (1998) 11.
6 D. M. Price, Proceedings of the 26th Conference of the North American Thermal Analyis Society (NATAS) Sept., 1998, p. 27.
7 M. Reading, Trends in Polymer Science, 1 (1993) 248.
8 J. E. K Schawe, Thermochim. Acta, 238 (1995) 1.
9 U. Jörimann, G. Widmann and R. Riesen, J. Therm. Anal. Cal., 56 (1999) 639.
10 J. A. Foreman, R. Riesen and G. Widmann, Thermal Trends, Vol. 5, No. 3, Summer 1998, p. 18.
11 N. G. McCrum, B. E. Read and G. Williams, Anelastic and Dielectric Effects in Polymeric Solids, Dover Publications, New York 1991, p. 169.
12 B. Wunderlich, Thermal Analysis, Academic Press, Boston 1990, p. 177ff.
13 M. Jaffe, Thermal Characterization of Polymeric Materials, 2nd Ed., E. A. Turi, ed., Academic Press, New York 1997, p. 1812.
14 G. Williams and D. C. Watts, Trans. Faraday Soc., 66 (1970) 80.